Hyperfine Interactions **136/137:** 743–747, 2001.

Study of Hyperfine Fields in $CeIn_3$ by Electronic Structure Calculations

M. V. LALIĆ[1,*], J. MESTNIK-FILHO[1,**], A. W. CARBONARI[1], R. N. SAXENA[1] and H. HAAS[2]

[1] *Instituto de Pesquisas Energéticas e Nucleares. P.O. Box 11049, 05422-970 São Paulo, Brazil*
[2] *Bereich Festörperphysik, Hahn-Meitner-Institut Berlin, D-14109 Berlin, Germany*

Abstract. Electronic band structure calculations for the $CeIn_3$ compound utilizing the full potential linearized augmented plane waves method were performed with the aim to compute the hyperfine fields acting on Ce and In atoms. The latter are found to be in reasonable agreement with the values measured at low temperatures. The 4f orbital contribution dominates the magnetic hyperfine field at Ce ions while the contact field is negligible due to an almost complete cancellation of valence and core contributions. A non-zero magnetic hyperfine field appears at In sites due to the spin-polarization of the 5p sub-shells through the hybridization with the extended 6s, 6p and 5d Ce states which, in turn, are spin-polarized by the Ce 4f states. No net magnetic moment at In is observed since the sum of its 5p sub-shell spins is zero. The 5p shell of In is responsible for the presence of an electric field gradient at In nuclei.

Key words: hyperfine fields, electronic structure, density functional calculations.

1. Introduction

$CeIn_3$ belongs to a class of compounds that exhibits some interesting and not completely understood physical phenomena such as intermediate valence, Kondo effect and superconductivity [1]. The Ce ion has an open 4f shell and thus a permanent magnetic moment which is usually preserved in the crystalline environment being screened from the outer conduction electrons. In $CeIn_3$ the Ce 4f moments are coupled by the Ruderman–Kittel–Kasuya–Yoshida (RKKY) interaction, resulting in an anti-ferromagnetic ordering of the Ce ions below $T_N = 10.2$ K. The moments are aligned in opposite directions in consecutive (1 1 1) planes of the cubic $CeIn_3$ lattice of $AuCu_3$ prototype. The measured saturation value of the Ce magnetic moment projection is $0.65 \pm 0.1\ \mu_B$ while the precise direction of the moments relative to the cell directions is not known [2].

The magnitudes of the hyperfine fields acting at both the Ce and In ions in $CeIn_3$ were recently measured by the TDPAC [3] and NQR [4] techniques. In the TDPAC study, using ^{140}Ce probes, the magnetic hyperfine field (MHF) at Ce nuclei was

* On leave from Institute of Nuclear Sciences 'Vinča', P.O. Box 522, 11001 Belgrade, Yugoslavia.
** Corresponding author. E-mail: jmestnik@net.ipen.br.

measured as a function of temperature down to 4.2 K at which point a value of 32.9 ± 0.1 T was obtained. From the NQR study a MHF of 0.4–0.5 T acting on In nuclei was found as well as an electric field gradient (EFG) of $V_{ZZ} = 11.6 \times 10^{21}$ V/m^2, using ^{115}In probes.

In the present work we performed an electronic structure calculation of $CeIn_3$ by means of the full potential linear augmented plane waves (FP-LAPW) method in order to have a deeper insight into these experimental findings. Special attention was devoted to questions that could not be answered by the experiments: (a) How the MHF is developed at the diamagnetic In sites; (b) What are the relative contributions of the contact, orbital and spin-dipolar characters of the MHF at both Ce and In ions; (c) Which electrons contribute to the EFG at In sites.

2. Details of the calculations

The aim of electronic structure calculations within the density functional theory is to determine the ground state electronic density of a solid, more specifically, the spin densities in our case. This is done by finding the spin densities that minimize the total energy which is, according to Hohenberg and Kohn [5], an exact functional of the density:

$$E[\rho] = T_s[\rho] + E_{ei}[\rho] + E_H[\rho] + E_{ii}[\rho] + E_{xc}[\rho].$$

Here, ρ denotes the electronic density (for electronic spins $[\rho] \rightarrow [\rho\uparrow, \rho\downarrow]$), $T_s[\rho]$ is the single particle kinetic energy, $E_{ei}[\rho]$ is the Coulomb interaction between electrons and nuclei, $E_{ii}[\rho]$ is the interaction between nuclei, $E_H[\rho]$ is the Hartree component of the electron–electron interaction and $E_{xc}[\rho]$ represents the exchange and correlation energy, usually approximated locally as the corresponding energy of a uniform electron gas (local density approximation, LDA). The latter is the most severe approximation in our calculations since it is expected that $CeIn_3$ has some higher degree of electronic correlation in comparison with ordinary compounds. Even the improved form for the exchange-correlation energy that was actually utilized, the generalized gradient approximation GGA [6], still does not account for high correlation effects.

A specially adapted wave functions set is utilized as a basis. Around each atom a sphere is drawn, inside which a linear combination of radial functions (solution of the radial Schrödinger equation) multiplied by spherical harmonics represents the basis wave functions. Outside these non-overlapping spheres (interstitial) the basis functions are plane waves constructed in a way to match the functions inside the spheres by value and first derivative at the surfaces. This special augmentation of the plane waves gives a very good representation of the charge densities and the potential near the atomic nucleus and hence, allows a good estimation of the hyperfine fields. The scalar relativistic approach for the valence states and fully relativistic treatment of core electrons were utilized. Spin-orbit effects are treated within a second variational approach.

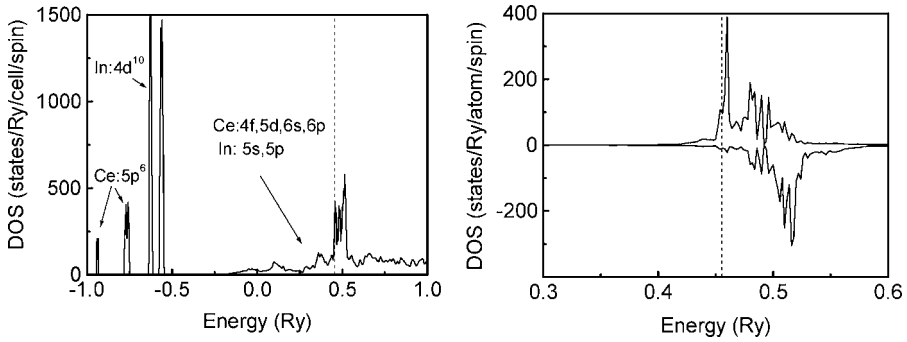

Figure 1. Total density of states (DOS) (left) and partial spin 'up' and spin 'down' DOS for Ce 4f states (right) in $CeIn_3$ compound. The dashed lines represent the Fermi level.

The self consistent band-structure calculations for $CeIn_3$ were performed by using the WIEN97 computer code which is based on the application of the FP-LAPW method [7]. The waves inside the atomic spheres were expanded up to $l_{max} = 6$, the plane wave cut-off was $K_{max} = 8.5/R_{MT}$ where $R_{MT} = 3$ a.u. was the chosen radius of the spheres and the spin densities were expanded up to $G_{max} = 14$. A tetrahedral mesh of 2000 k-points in the Brillouin zone (or 182 in its irreducible wedge) was utilized to perform a k-space integration. The $5s^2 5p^6 4f^1 5d^1 6s^2 6p^0$ states of Ce and $4d^{10} 5s^2 5p^1$ of In were treated as valence states. The calculations of MHFs, including relativistic effects, implemented in the WIEN97 code, are performed following the formulae from ref. [8]. A collinear magnetic structure was considered.

3. Results and discussion

Three fully self-consistent band structure calculations for $CeIn_3$ were performed for three different orientations of the magnetization axis, i.e., the [1 0 0], [1 1 0] and [1 1 1] directions. The resulting differences in the total energy and in the MHF were respectively $\sim 10^{-5}$ Ry and $\sim 5\%$, preventing us to determine which configuration should be preferable and hence, in the following we will discuss only the results obtained considering [1 1 1] as the direction for the magnetization axis.

The resulting total density of states (DOS) and the partial spin-up and spin-down DOS from Ce 4f states in $CeIn_3$ compound are presented in Figure 1. The Ce 4f, 5d, 6s, 6p and In 5s, 5p states form a broad band around the Fermi level, whereas the remaining valence states keep the atomic-like characters but are split due to the crystal-field and spin–orbit perturbation.

The spin polarization of the Ce 4f states is evident from Figure 1 and its calculated population of 1.039 electrons indicates that the valence ground state of Ce in $CeIn_3$ compound is Ce^{+3}. The spin magnetic moment at the Ce atom was found to be 0.708 μ_B, mostly coming from the 4f shell (0.639 μ_B). In addition, the Ce atom develops a significant orbital magnetic moment of -0.531 μ_B, also mainly

Table I. Comparison of FP-LAPW results for MHFs in $CeIn_3$ compound with the experimental values, together with the theoretical decomposition of the MHFs. Only absolute values of MHFs were measured

	|MHF (T)| Experiment	MHF (T) FP-LAPW	Contact field (T)	Orbital field (T)	Spin-dipolar field (T)
Ce	32.9 ± 0.1	-25.05	2.20	-27.74	0.49
In	0.4–0.5	-0.91	-0.04	-0.16	-0.71

from the 4f shell. Thus the total magnetic moment on Ce resulted to be 0.177 μ_B, in disagreement with the neutron scattering result, a fact that was attributed to the failure of the LDA discussed above. No net magnetic moment was found at the In position but it was found that its 5p sub-shells are spin-polarized in a way to cancel the overall 5p shell polarization, i.e., the spin populations of the p_x, p_y, p_z orbitals differ for spin-up and spin-down respectively by 0.006, 0.004 and -0.010 electrons.

The results for the magnetic hyperfine fields are presented in Table I. At the Ce site the MHF is dominated by the orbital contribution from the 4f shell. The contact field is small in comparison with the orbital field due to the fact that there is an almost complete cancellation between the valence and core contributions. The valence contribution arises from the 6s magnetic moment (0.003 μ_B) leading to a contact field of +24.8 T whereas the core electrons contribute with -22.6 T. The reasonably good agreement of the calculated and the experimental Ce MHF values contrasts with the poor agreement of the corresponding magnetic moments. The origin of the discrepancy is not known, but, as the dominating part of the Ce MHF comes from its 4f orbital moment, it suggests the possibility that the orbital contribution to the magnetic moment is determined correctly whereas the same is not true for the spin counterpart.

A small MHF at In positions also resulted from our calculations, with a dominant spin-dipolar character. It was found that both spin-dipolar and orbital fields originate completely from the In 5p valence shell through the spin-polarization of its sub-shells. The reason for this polarization is the existence of a large 4f magnetic moment at the Ce atom which polarizes the more extended 6s, 6p, 5d states of Ce and these hybridize with the 5p shells of the neighboring In atoms causing the polarization of their 5p sub-shells. A different approach to understand the appearance of a MHF at In sites is given in ref. [9], where it is shown that In 5s shell could become spin-polarized if a non-collinear magnetic structure in $CeIn_3$ is considered. In this case an additional MHF at In nucleus with the Fermi contact field character can be expected.

The results for the electric field gradient at In sites are presented in Table II. The 5p contribution is predominant whereas the small d contribution results from

Table II. Main component of the EFG tensor at In sites in $CeIn_3$ compounds and the decomposition of the valence contribution, in units of 10^{21} V/m^2

	$\|V_{ZZ}\|$ Experiment	V_{ZZ} FP-LAPW	Valence contrib.	s–d contrib.	p–p contrib.	d–d contrib.
In	11.6	12.49	12.54	−0.05	13.26	−0.67

an extension of the tails of the wave functions arriving from neighboring spheres into the In atomic sphere. The spin-polarization of the In 5p sub-shells do not have any effect on the EFG since it was observed that both the spin-up and spin-down charge densities lead to the half of the EFG value. It was shown that this effect comes from the fact that the spin-polarization of the 5p sub-shells of In occur at relatively large distance from the In nucleus, larger than the radius at which the first node of the 5p wave-functions occurs [10].

Acknowledgements

Partial support was provided by the Fundação de Amparo à Pesquisa do Estado de São Paulo (FAPESP). M. L. V. thankfully acknowledges the support provided by FAPESP in the form of a research fellowship.

References

1. Bushow, K. H. J., *Rep. Prog. Phys.* **42** (1979), 1373.
2. Lawrence, J. M. and Shapiro, S. M. *Phys. Rev. B* **22** (1980), 4379.
3. Carbonari, A. W., Mestnik-Filho, J., Saxena, R. N. and Saitovitch H., *Hyp. Interact.* **133** (2001), 33.
4. Kohori, Y., Inoue, Y., Kohara, T., Tomba, G. and Riedi, P. C., *Phys. B* **103**, (1999), 103.
5. Hohenberg, P. and Kohn, W., *Phys. Rev. B* **136** (1964), 864.
6. Perdew, J. P., Burke, S. and Ernzerhof, M., *Phys. Rev. Let.* **77** (1996), 3865.
7. Blaha, P., Schwarz, K. and Luitz, J. *WIEN97. A Full Potential Linearized Augmented Plane Wave Package for Calculating Crystal Properties*, K. Schwarz, Tech. Univ. Wien, Wienna, 1999. ISBN 3-9501031-0-4. Updated version of Blaha, P., Schwarz, K., Sorantin, P. and Trickey, S. B., *Comp. Phys. Comm.* **59** (1990), 399.
8. Blügel, S., Akai, H., Zeller, R. and Dederichs, P. H., *Phys. Rev. B* **35** (1987), 3271.
9. Demuynck, S., Sandratskii, L., Cottenier, S., Meersschaut, J. and Rots, M., *J. Phys. Condens. Matter* **12** (2000), 4629.
10. Blaha, P., Schwarz, K. and Dederichs, P. H., *Phys. Rev. B* **37** (1988), 2729.